Bioelectrochemistry 153 (2023) 108467

Contents lists available at ScienceDirect

Bioelectrochemistry

journal homepage: www.journals.elsevier.com/bioelectrochemistry

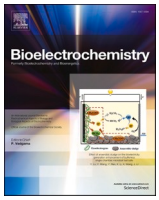

Rapid identification of *in vitro* cell toxicity using an electrochemical membrane screening platform

Yvonne Kohl [a,1], Nicola William [b,1], Elisabeth Elje [c,d], Nadine Backes [a], Mario Rothbauer [e], Annamaria Srancikova [f], Elise Rundén-Pran [c], Naouale El Yamani [c], Rafi Korenstein [g], Lea Madi [g], Alexander Barbul [g], Katarina Kozics [f], Monika Sramkova [f], Karen Steenson [b], Alena Gabelova [f], Peter Ertl [e,h], Maria Dusinska [c], Andrew Nelson [b,*]

[a] *Fraunhofer Institute for Biomedical Engineering IBMT, Joseph-von-Fraunhofer-Weg 1, Sulzbach 66280, Germany*
[b] *School of Chemistry and Faculty of Engineering and Physical Sciences, University of Leeds, Leeds LS2 9JT, United Kingdom*
[c] *NILU-Norwegian Institute for Air Research, Department for Environmental Chemistry, Health Effects Laboratory, Instituttveien 18, Kjeller 2007, Norway*
[d] *Faculty of Medicine, Institute of Basic Medical Sciences Department of Molecular Medicine, University of Oslo, Sognsvannsveien 9, Oslo 0372, Norway*
[e] *Institute of Applied Synthetic Chemistry, Vienna University of Technology, Getreidemarkt 9, 1060 Vienna, Austria*
[f] *Department of Nanobiology, Cancer Research Institute, Biomedical Research Center of the Slovak Academy of Sciences, Dubravska Cesta 9, Bratislava 84505, Slovakia*
[g] *Department of Physiology and Pharmacology, Sackler Faculty of Medicine, Tel Aviv University, Tel Aviv, 69978, Israel*
[h] *Institute of Chemical Technologies and Analytics, Vienna University of Technology, Getreidemarkt 9, 1060 Vienna, Austria*

ARTICLE INFO

Keywords:
Electrochemical membrane sensor
Intercalibration
Toxicants
Acute cell viability
Comet assay
Colony forming efficiency assay

ABSTRACT

This study compares the performance and output of an electrochemical phospholipid membrane platform against respective *in vitro* cell-based toxicity testing methods using three toxicants of different biological action (chlorpromazine (CPZ), colchicine (COL) and methyl methanesulphonate (MMS)). Human cell lines from seven different tissues (lung, liver, kidney, placenta, intestine, immune system) were used to validate this physico-chemical testing system. For the cell-based systems, the effective concentration at 50 % cell death (EC_{50}) values are calculated. For the membrane sensor, a limit of detection (LoD) value was extracted as a quantitative parameter describing the minimum concentration of toxicant which significantly affects the structure of the phospholipid sensor membrane layer. LoD values were found to align well with the EC_{50} values when acute cell viability was used as an end-point and showed a similar toxicity ranking of the tested toxicants. Using the colony forming efficiency (CFE) or DNA damage as end-point, a different order of toxicity ranking was observed. The results of this study showed that the electrochemical membrane sensor generates a parameter relating to bio-membrane damage, which is the predominant factor in decreasing cell viability when *in vitro* models are acutely exposed to toxicants. These results lead the way to using electrochemical membrane-based sensors for rapid relevant preliminary toxicity screens.

Abbreviations: **CCM**, Cell culture media; **CFE**, Colony forming efficiency; **COL**, Colchicine; **CPZ**, Chlorpromazine; **DNA**, Deoxyribonucleic acid; **DMEM**, Dulbecco's Modified Eagle's medium; **DMSO**, Dimethylsulphoxide; **DOPC**, Dioleyl phosphatidylcholine; **EC50**, Effective concentration at 50 % cell death; **FCS**, Foetal calf serum; **FBS**, Foetal bovine serum; **Hg**, Mercury; **HPLC**, High performance liquid chromatography; **HTP**, High throughput; **IAM**, Immobilised artificial membrane; **LoD**, Limit of detection; **MIE**, Molecular initiating event; **MMS**, Methyl methanesulphonate; **MTT**, 3-(4,5-dimethylthiazol-2-yl)-2,5-diphenyltetrazolium bromide; **NMR**, Nuclear magnetic resonance; **PBS**, Phosphate buffered saline; **PS**, Penicillin/Streptomycin; **Pt**, Platinum; **RCV**, Rapid cyclic voltammograms; **SB**, Strand breaks; **SD**, Standard deviation; **SN2**, Second order nucleophilic substitution.

* Corresponding author.
E-mail addresses: yvonne.kohl@ibmt.fraunhofer.de (Y. Kohl), n.william@leeds.ac.uk (N. William), eel@nilu.no (E. Elje), mario.rothbauer@tuwien.ac.at (M. Rothbauer), annamaria.srancikova@savba.sk (A. Srancikova), erp@nilu.no (E. Rundén-Pran), korens@tauex.tau.ac.il (R. Korenstein), lmadi@tauex.tau.ac.il (L. Madi), abarbul@tauex.tau.ac.il (A. Barbul), katarina.kozics@savba.sk (K. Kozics), monika.sramkova@savba.sk (M. Sramkova), k.a.steenson@leeds.ac.uk (K. Steenson), alena.gabelova@savba.sk (A. Gabelova), peter.ertl@tuwien.ac.at (P. Ertl), mdu@nilu.no, ney@nilu.no (M. Dusinska), a.l.nelson@leeds.ac.uk (A. Nelson).
[1] Equally contributed.

https://doi.org/10.1016/j.bioelechem.2023.108467
Received 21 February 2023; Received in revised form 28 April 2023; Accepted 15 May 2023
Available online 19 May 2023

1. Introduction

With the increasing cultural and regulatory changes in recent years, there is a great demand to replace animal studies in the field of toxicological testing of chemicals with high throughput (HTP) *in vitro* and *in silico* models for a better understanding of the mode of action and the pathways leading to an adverse outcome [1]. Cell membrane integrity is one of the key initial events in cellular toxicity and constitutes a minimal or "baseline" toxicity of every chemical [2]. The entry and distribution of chemicals in biological systems is strongly determined by biomembranes [3].

The logarithm of the octanol–water partition coefficient (log *P*) for non-ionisable compounds and log *D* for ionisable compounds are often used as parameters to estimate the partitioning of solutes into biomembranes [4,5]. For many chemicals, octanol is not an appropriate analogue for the anisotropic structure and complex molecular interactions within the biological membrane [6]. Nevertheless, log *P* and log *D* are used as standardized parameters to predict toxicological potential. However, there are some biomembrane models and techniques providing a more accurate estimate of the distribution in biomembranes. These include: liposome water partitioning [4], *in vitro* studies [7], nuclear magnetic resonance (NMR) [8], surface plasmon resonance spectroscopy [9], microscopic techniques [10], and theoretical molecular simulations [11,12]. However, these methods are often time consuming, cost intensive and rarely suitable for routine HTP screening. Over the last thirty years, a new membrane model has been developed that involves the use of specialised columns on a high performance liquid chromatography (HPLC) platform, and which consists of dialkyl phospholipids covalently bound to porous silica particles in a column. The phospholipid layer acts as an immobilised artificial membrane (IAM) and can be considered as stationary phase. The phospholipid phase affinity of the compound of interest is then estimated from the retention factor, which can be converted to a membrane-water partition value and has been found to correlate well with values obtained by liposome-water partitioning [13,14]. In fact, the association of a compound with the IAM phospholipid layer has been shown to be directly related to its log *P* [13,14]. The drawback associated with the IAM platform is that it only measures membrane assumed biomembrane affinity. It provides very little information on the biomembrane damaging propensity of a specific compound or pharmaceutical. Since biomembrane modification and damage features are strongly involved in molecular initiating events (MIE) of any toxicological process, other HTP membrane screening platforms are required which can measure this. In addition, IAM chromatography is not applicable to screening nanomaterial and particle dispersions due to fouling of the HPLC column. The Hg-supported dioleoyl phosphatidylcholine (DOPC) monolayer platform [15–18] using electrochemical interrogation has been employed as one successful biomembrane model. This model has recently been transferred to a HTP platform [19,20] and has been developed to screen organic compounds [21] and nanomaterial dispersions [22,23] in water. However, what it precisely measures in terms of compound-biomembrane interaction is still uncertain. Indeed, a recent study comparing the screening of a series of low molecular weight organic compounds, using both the electrochemical membrane and the IAM platforms showed that the electrochemical screen measures molecular properties in addition to lipid membrane affinity [24].

This present study was carried out to further investigate which bioactive property in addition to apolarity or hydrophobicity, the electrochemical membrane screen actually measures and how this can be related to the MIE of a particular compound. In the following, three demonstrator compounds of well-known biologically activity have been screened using the electrochemical membrane platform. In parallel, the three compounds were tested in routine toxicity assays using seven different *in vitro* models by five different laboratories respectively. Generally, cell viability measurements were used to determine the acute toxicity of the compounds. Additionally, experiments were carried out to examine the compounds' effect on (a) cellular proliferation (reflected by the cell colony forming efficiency (CFE)) and (b) genotoxicity of the compounds by the comet assay.The three compounds used in this study were chlorpromazine (CPZ), colchicine (COL) and methyl methanesulphonate (MMS). CPZ had previously been shown to be active towards the supported phospholipid layer sensor element [21,25]. This established biomembrane activity of CPZ is related to its apolarity and high log *P* value as well as to its tricyclic structure [25], which sterically favours biomembrane penetration. The side group terminating in a nitrogen grouping will facilitate a vertical orientation in the phospholipid layer by associating with the phospholipid polar groups through H-bonding. CPZ is a known antipsychotic [26] with antimalarial properties [27] and is highly lipid membrane [28] and biomembrane [29] active. MMS' principal biological activity is as an alkylating agent [30] that alkylates the DNA base pairs, damaging DNA [31,32] through its mutagenic [33] properties. The reactive methyl group of MMS can attack cellular targets including DNA by nucleophilic substitution through the SN2 mechanism [34], although a more general effect on cell necroptosis has been observed [35]. Evidence has also been shown that MMS activity is directed at proteins and indeed lipids [36]. In this study, MMS was chosen as a test compound to assess: (a) whether it had any effect on phospholipids through its alkylating activity, (b) to what extent the MMS influenced viability of the cell line based models, and finally (c) to apportion the mechanisms of possible MMS toxicity to DNA and to the interaction of MMS with the cellular components including the cell membrane. On a molecular level, COL can be described as an antimitotic drug, blocking the mitotic activity of cells in the metaphase part of the cell cycle [37]. Specifically, COL binds to tubulin, forming complexes which bind to microtubules [38] and this prevents their elongation. At low concentrations, COL stops microtubule growth [38–40] and, at elevated concentrations, COL causes the depolymerisation of microtubules [40]. Although the tubulin structure is a highly complex protein, the tricyclic nature of COL containing one aromatic moiety predicted a degree of interaction with lipids, which has in fact been previously observed [41]. These three compounds were chosen due to their widely different biological activities as detailed above. They were used in this study to characterise exactly the biological activity to which the electrochemical sensor responded and whether this response was selective to a particular mode of action. All chemical compounds are potentially toxic to cells and their toxicity depends on their concentration/dose and mode of action.

The aim of this study therefore was to assess the extent of interaction of the three test compounds with the phospholipid monolayer sensor element and then evaluate how significant this activity was compared to the compounds' toxicity to cell cultures. If this study could show that the electrochemical sensor generates a parameter relating to biomembrane damage, these results could lead the way to using the electrochemical membrane-based sensors for rapid, cell-free, acute toxicity screens.

2. Materials and methods

2.1. Materials

CPZ, COL and MMS were obtained from Sigma-Aldrich. Stock solutions were prepared in acetone and diluted to working solutions in KCl electrolyte or cell culture medium. The electrolyte used throughout the experiments was 0.138 mmol/cm^3 NaCl and 2 μmol/cm^3 KCl buffered at pH 7.4 with 11.9 μmol/cm^3 phosphate (subsequently referred to as PBS in the following text). The PBS was of analytical grade and purchased from Sigma-Aldrich (Vienna, Austria; Gillingham, UK and Oslo Norway). PBS for *in vitro* studies and cell culture media was purchased from Fisher Scientific (Vienna, Austria; Gillingham, UK and Oslo, Norway), Gibco BRL (Paisley, UK) or Sigma-Aldrich (Steinheim, Germany and Rehovot, Israel). The DOPC was obtained from Avanti Polar Lipids Inc. (Alabaster, AL, US) and was $>$ 99 % pure. By carefully shaking DOPC with PBS, the 0.25 mmol mL^{-1} DOPC dispersion for electrode coating

was prepared. All other reagents were of analytical grade and purchased from Sigma-Aldrich. The microfabricated platinum electrodes [20,21,42,43] were supplied by the Tyndall National Institute (Cork, Ireland). Hg was electrodeposited on the Pt disc of radius 0.480 mm to give a Pt/Hg electrode as described previously [20,21,42,43]. All materials needed for CFE assay and genotoxicity assay were purchased from ThermoFisher (Waltham, MA, USA) and Sigma-Aldrich (Gillingham, UK and Oslo, Norway) [44].

2.2. Methods

2.2.1. Electrochemical biomembrane screening platform

Principle

As a biomembrane mimic, a DOPC monolayer is deposited on the Hg electrode on the prepared Pt support. These layers undergo potential-induced phase transitions characterised by two sharp capacitance current peaks (voltametric) peaks, 1 and 2 respectively, as shown in Fig. 1**a** [20,21,42,43]. These two peaks correspond to the penetration of electrolyte into the layer and the reorganisation of the monolayer to form bilayer patches, respectively [45–47]. Changes in these capacitance peaks are equivalent to changes in the structure of the monolayer [20,21,42,43]. The interaction of the test substance with the monolayer selectively and systematically influences the capacitance-current–potential profile [22–24]. An interaction of the test substance with the polar groups of the DOPC is reflected in a depression of the two peaks [22] while an increase in the baseline of the capacitance current reflects the association of a polar compound with the apolar region of the DOPC layer and/or its disruption [23,24]. The reason for the latter effect is that the low value of baseline capacitance current is representative of the ordered DOPC layers on the electrode with the low dielectric apolar lipid tails adjacent to the electrode surface. When this low dielectric region is penetrated by a higher dielectric compound, the average dielectric constant of this region increases leading to an increase in the baseline capacitance current [15,17,23,24]. A potential shift in the capacitance current peaks indicates a change in the potential profile across the layer caused by the interaction of the compound with the layer [48]. A monolayer disordering is shown as a broadening of the peaks [23,24]. Other research groups followed a similar approach, but not in rapid online screening format [49–51].

Apparatus and procedure

Mohamadi et al. [21] describes all details of the platform and procedure used in this study. The interactions of the test substances with the DOPC monolayer are monitored by rapid cyclic voltammograms (RCV), while cycling the electrode potential from −0.4 to −1.2 V for 600 s during compound exposure. RCV plots were generated from the electrochemical experiments Each RCV plot is a unique "fingerprint" characterising the interaction of each test compound with the DOPC monolayer. To obtain a quantitative estimate of the effects of each test substance on the DOPC layer, the limits of detection (LoD) for the compound in PBS were calculated. LoD is the lowest concentration of the test substance in PBS resulting in a statistically significant effect on the properties of the monolayer. The LoD represents a quantitative, analytical output of the RCV technology. Its experimental determination has been described previously [21]. Due to the dynamic, induced mobility of the sensor element, the RCV results should refer to the mode in which the compound/DOPC association influences the DOPC monolayer assembly. Indeed –log LoD can be taken as a metric describing the ability of the compound-DOPC interaction to modify the DOPC layer organisation.

Cell culture and *in vitro* assays

Cell culture

Seven human cell lines of different organ origins were used: A549 (lung epithelial), BeWo b30 (placental choriocarcinoma), Caco-2 TC7 (colon epithelial), HEK293 (embryonic kidney), HepG2 (human hepatocarcinoma), TH1 (renal proximal tubule epithelial) and THP1 (human monocytes). A549 cells (ATCC CCL-185) were cultured as previously described in Kohl *et al.* [52]. BeWo b30 cells (kindly provided by Dr. Berthold Huppertz, Medical University of Graz, Austria) were cultivated as reported previously [53]. Caco-2 TC7 cells (a kind gift from Monique Rousset, INSERM U178, Villejuif, France), were cultured in DMEM as described previously [54]. HepG2 cells, provided from the ECACC (European Collection of Authenticated Cell Cultures, #85011430, Salisbury, United Kingdom), were cultured as previously explained in Elje *et al.* [44]. TH1 cells (Kerafast, #ECH001) were cultivated as described in Sramkova *et al.* [55]. THP1 cells (ECACC #88081201) were cultured in Roswell Park Memorial Institute (RPMI 1640) medium supplemented with 10 % FBS and antibiotics (penicillin 100 U/ml and streptomycin 100 μg/ml), and HEK293 cells (ECACC #85120602) were cultivated in Eagle's Minimum Essential Medium (EMEM), supplemented with 10 % foetal bovine serum (FBS), and antibiotics (penicillin 100 U/ml and streptomycin 100 μg/ml). All cells were cultivated in a humidified atmosphere at 37 °C and 5 % CO_2.

Cell viability assays AlamarBlue™ and PrestoBlue™

Cell viability was determined by AlamarBlue™ assay [56] (DAL1100, Thermo Fisher Life Technologies Corporation, Eugene Oregon USA or DAL1025, Fisher Scientific, Schwerte, Germany) or PrestoBlue™ assay [57] (A13261, Thermo Fischer Scientific (Vienna, Austria). or DAL1100, Thermo Fisher Life Technologies Corporation, Eugene Oregon USA) according to the manufacturer's operating procedures. The reagent solutions contain a non-fluorescent cell permeant molecule, which when chemically reduced by the metabolic activity of cells, turns into a highly fluorescent coloured dye. Both the colour change and the change in fluorescence allows for the direct measurement of cell metabolic activity. The cells were seeded in 96-well plates, 24 hrs before exposure, at concentrations of 10,000 cells/well for A549, Caco-2 TC7 and TH1; 20,000 cells/well for HepG2 and THP1; and

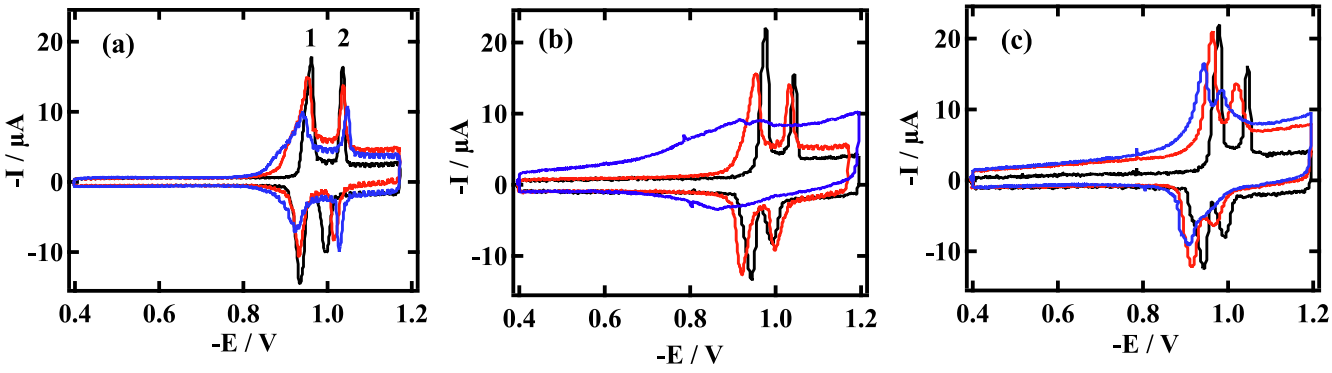

Fig. 1. Representative rapid cyclic voltammograms (RCVs) recorded from a DOPC coated Pt/Hg (black line) monolayer platform in the presence of, (a) 0.001 (red line) and 0.3 (blue line) nmol/cm^3 CPZ, (b) 7 (red line) and 75 (blue line) nmol/cm^3 MMS and (c) 3 (red line) and 20 (blue line) nmol/cm^3 COL in PBS at pH 7.4. Capacitance current peaks 1 and 2 marked on (a).

17,000 cells/well for BeWo b30. Concentrations of the test compounds and solvents are summarised in Table 1. The cells were exposed to the test compounds for durations of 3, 4.5 and 24 hrs. Cell viability was measured by reading the fluorescence intensity in a microplate reader according to the manufacturer's operating procedures. Control values (i.e. culture medium with AlamarBlue™/PrestoBlue™ solution alone, without cells) were extracted from all measurements, and viability was calculated relative to a negative control, i.e. cells exposed to cell culture medium only, which was set to 100 %. Two to three replicates were included per condition within each experiment, and 2–3 independent experiments were performed.

Colony forming efficiency (CFE) assay

The CFE assay measures cell viability by colony formation after exposure of single cells [58]. A549 cells were seeded in 6-well plates at a density of 50 cells per well, and exposed to different concentrations of the test compounds (Table 1) continuously for 10–12 days, to allow formation of colonies according to the protocol published by El Yamani *et al.* (2017) [59]. Six replica wells were used for each condition within each experiment, and three independent experiments were performed. The negative control was cell culture medium, whilst the positive control was 10 nM staurosporin (Merck, Rehovot, Israel). Cell viability was expressed as % CFE relative to the negative control set at 100 %. Solvent control (H_2O or PBS) was also included at the concentration corresponding to the highest applied concentration of the test substance, and no significant effect was seen (results not shown). In the CFE assay, suspension cell-lines cannot be used, so the assay can only be used with adherent cell lines such as A549. In addition, not all adherent cell-lines are suitable due to the two following factors:- (a) they have low or limited cloning efficiency, and/or (b) they do not form clear colonies which can be analysed. The A549 cell-line was therefore used in the CFE assay, since it has the highest cloning efficiency.

Genotoxicity assay

The miniaturised alkaline version of the comet assay was used to measure genotoxicity by DNA strand breaks and apurinic and apyrimidinic sites. The comet assay is a well-known, sensitive technique for the detection of different types of DNA damage in single eukaryotic cells [60]. It involves embedding cells (previously exposed to the test compound) in a low melting point (LMP) agarose gel, lysis of the cells in alkaline conditions and electrophoresis of the nuclei. The procedure of the alkaline comet assay has been published in Dusinska et al., [61], Balintová et al., [62] and El Yamani et al., [63] and most recently in Nature Protocols [64]. Median DNA tail intensity, proportional to the number of strand breaks (SBs), was calculated as a measure of DNA SBs. Medians were averaged from duplicate gels per cell culture. Three independent experiments were performed. The positive control for SBs was H_2O_2 exposure (100 μM for 5 min) as explained in detail in Dusinska et al., [61], Elje et al., [44] and El Yamani et al., [63].

A summary of all *in vitro* toxicity tests performed in the presented study for the validation of the electrochemical membrane screening device are displayed in Tables 1 and 2.

Statistics

Data are presented as mean ± SD from at least three independent experiments with triplicates per sample. The differences between treated samples and untreated control were evaluated by the Student's *t*-test and one-way analysis of variance (ANOVA). The threshold of statistical significance was set to $p < 0.05$.

3. Results and discussion

This study aims to validate the performance of the novel rapid membrane screen, the Hg-supported dioleoyl phosphatidylcholine (DOPC) monolayer platform, for applicability to the toxicity screening of chemicals and pharmaceuticals. Validation was performed by comparing the electrochemical screen to cyto- and genotoxicity data generated by exposure of seven cell lines to the test compounds CPZ, MMS and COL.

3.1. Compounds screened

The three test compounds CPZ, MMS and COL have widely different chemical structures as well as different log *P*, pK_a and log *D* values at pH 7.4 (log $D^{pH7.4}$) (Table 3). This will account for the wide difference in their biological activities. The log *D* value at pH 7.4 (log $D^{pH7.4}$) for CPZ and COL was estimated from $\log D^{pH7.4} = \log P - \log [1 + 10^{(pKa-7.4)}]$ [65]. The MMS was not ionisable and it can be assumed that the log $D^{pH7.4}$ value is identical to its log *P* value.

3.2. Electrochemical screening of CPZ, MMS and COL

With the Hg-supported dioleoyl phosphatidylcholine (DOPC) monolayer platform, RCVs were monitored following the interaction of the DOPC monolayer biomembrane model with increasing concentrations of the selected test compounds (Fig. 1a-c).

Interaction of CPZ with DOPC depresses and modifies the two capacitance current peaks but an overall degradation of the peak structure is not observed and only the baseline at negative potentials is incorporated within the capacitance current peak (Fig. 1**a**). A modification, but not disorganisation of the layer structure, can be interpreted from this. Interaction of MMS with DOPC has the effect of depressing both capacitance current peaks and at higher concentrations effecting an increase in the baseline current. This increase indicates a significant penetration of MMS into the layer structure (Fig. 1**b**). Interaction of COL with DOPC generally degrades, broadens and merges the capacitance current peaks. This indicates that COL both modifies and degrades the layer structure (Fig. 1**c**). A plot of capacitance peak 1 current as percentage of control versus the solution concentration of the three compounds shows that the DOPC layer is very much more sensitive to CPZ interaction than to COL and MMS interaction (Fig. 2**a**). These data were transformed to peak suppression % versus solution concentration plots (Fig. 2b and c) used for LoD estimation and values are listed in **Table S1**. The method of calculation of the LoD is described in the following. The plots of voltammetric peak height suppression versus solution concentration are fitted to a Langmuir type equation where the % peak depression (y) is equivalent to the extent of interaction of the compound in solution, of concentration (C), with the DOPC layer. The equation used is:-

$$y = aC/(100 + bC) \quad (1)$$

where a and b are coefficients having the units: % × cm^3/nmol and cm^3/nmol respectively.

The LoD is estimated from Eq. (1) by substituting three times the coefficient of variation of the control capacitance peak 1 current as y into equation (1) and solving for C as the LoD. The error of the LoD

Table 1
Summary of the settings of the electrochemical membrane screening. Assay solvent was PBS. COL: Colchicine, CPZ: Chlorpromazine, DOPC: Dioleyl phosphatidylcholine, MMS: Methyl methanesulphonate, PBS: Phosphate buffered saline.

Assay (measurement)	Assay Endpoint	Sensor Element	Delivery concentration [nmol/cm^3]	Delivery solvent	Exposure time
Electrochemical biomembrane screening	Phospholipid layer disruption	DOPC monolayer	0.001 to 3 (CPZ) 3.125 to 75 (MMS) 3.125 to 75 (COL)	PBS	10 min

Table 2
Summary of the *in vitro* cell culture experiments used for the validation of the electrochemical membrane screening platform. Assay solvent was cell culture medium. CCM: Cell culture medium, CFE: Colony forming efficiency, COL: Colchicine, CPZ: Chlorpromazine, DMSO: Dimethylsulphoxide, FCS: Foetal calf serum, FBS: Foetal bovine serum, MMS: Methyl methanesulphonate, PBS: Phosphate buffered saline, PS: Penicillin/Streptomycin.

Assay (measurement)	Assay Endpoint	Cell line	Delivery concentration [nmol/cm^3]	Delivery solvent	Exposure time
AlamarBlue™ (Fluorescence)	Cell viability	A549 HepG2 HEK293 TH1 THP1	0 to 1000 (CPZ, MMS, COL)	H_2O (CPZ) PBS (MMS) PBS (COL)	3 hrs, 24 hrs
PrestoBlue™ (Fluorescence)		Caco-2 TC7	0 to 500 (CPZ, MMS, COL)		
		BeWo b30	0 to 1000 (CPZ, MMS, COL)	H_2O (CPZ) CCM (MMS) CCM(COL)	4.5 hrs 24 hrs
CFE (cell number of colonies)		A549	0 to 300 (CPZ, MMS, COL)	H_2O (CPZ) DMSO + PBS (MMS) PBS (COL)	10–12 days
Comet	Genotoxicity	A549 HEK293 HepG2 TH1 THP1	0 to 1000 (CPZ, MMS, COL)	H_2O (CPZ) DMSO + PBS (MMS) PBS (COL)	3 hrs, 24 hrs

Table 3
Structure, log *P*, pK_a and log $D^{pH7.4}$ values of the test compounds CPZ, MMS, and COL used in this study for validation.

Compound	Structure	Log *P*	pK_a	Log $D^{pH7.4}$
CPZ	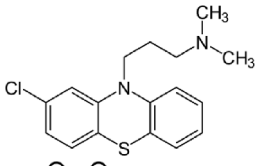	5.41 [66]	9.2 [66]	3.60
MMS	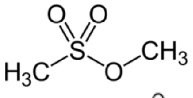	−0.7 [67]		−0.7
COL	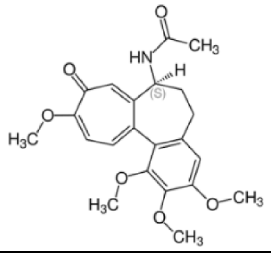	1.03 [37]	1.85 [68]	1.03

estimation was taken as the sum of the errors of both coefficients, a and b, in the fit of equation (1) to the data. The coefficients for the three fits to the calibration curves respectively are listed in the SI, Table S2. In fact, quantitatively the interaction ranking order in terms of the LoD values is CPZ: $4.2 \times 10^{-5} \pm 8.55 \times 10^{-6}$, < MMS: 0.27 ± 0.132, < COL: 0.77 ± 0.257 nmol/cm^3. Consequently, CPZ is ~6400 times more likely to modify the DOPC layer organisation than MMS, whereas MMS has nearly three times the tendency for DOPC layer modification over COL. Thus although CPZ at very low solution concentration does not appear to penetrate the DOPC layer, CPZ does interact with the polar heads of the DOPC monolayer, significantly affecting their conformation. Certainly if its concentration was increased by a further factor of ten, the CPZ would fully penetrate the layer which would be disrupted to a far greater extent..

3.3. Cell viability screening of CPZ, MMS and COL in human in vitro models

Seven different cell lines, of different tissue origin, were exposed to the test compounds CPZ, MMS or COL for 3 and 24 hrs and cell viability was measured using the AlamarBlue™/PrestoBlue™ assay [56,57]. These *in vitro* assays exploit the ability of cells to metabolically reduce AlamarBlue™/PrestoBlue™ reagent into a fluorescent dye whereby the fluorescent intensity is proportional to the viability of the cells. The effect of the three compounds on the viability of. three representative cell cultures (HEK293, Caco-2 TC7 and THP1) versus test compound

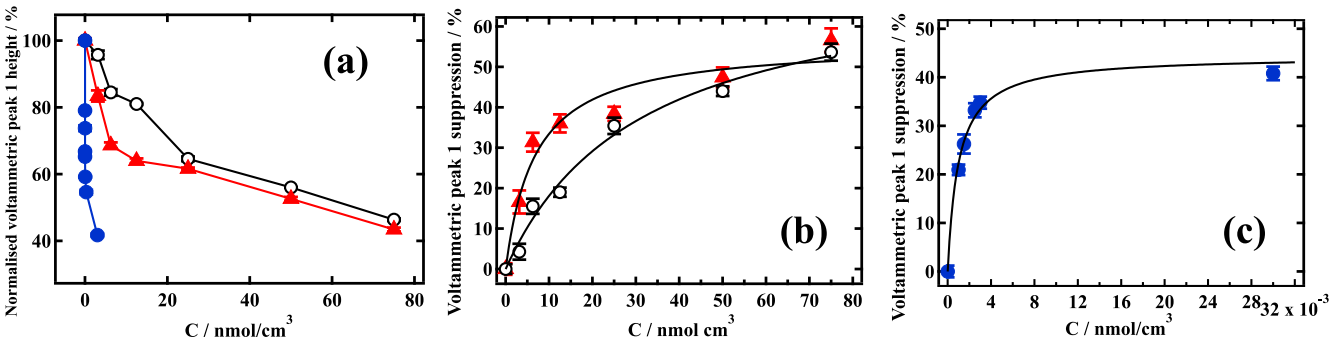

Fig. 2. Electrochemical assay: Plots of (a) capacitance peak 1 current as percentage of control, (b), (c) % suppression of the capacitance peak 1 current, versus the solution concentration of the following compounds in PBS: COL: unfilled black circles, MMS: red triangles, CPZ: blue circles. Data from n = 3 assays are shown as mean ± SD. Fit to Eq. (1) in (b) and (c): black line.

concentrations is shown in Fig. 3. The dose–response curves obtained for the cells A549, THP1, TH1 and BeWo b30 are similar to those displayed in Fig. 3 and are displayed in **Fig. S1**. Most notable is that the order of toxicity effectiveness to the *in vitro* models mirrors that shown by the DOPC monolayer sensing platform namely CPZ > MMS > COL. Although the full response to CPZ is observed within 3–4 hrs of incubation, the response of the cell cultures to MMS is not fully realised until 24 hrs after initial exposure.

For the cell-based systems, EC_{50} values were calculated from all dose–response curves. The relation between LoD and EC_{50} values are shown in Fig. 4. This displays –log EC_{50} and –log LoD values after 24 hrs exposure of HEK293, THP1 and TH1 cell lines and 2–3 min exposure of the DOPC sensor element to the three compounds respectively, versus the compound log $D^{pH7.4}$. It is noted that the acute cell viability EC_{50} values for MMS and COL, and CPZ are >500 and ~10^6 times respectively less sensitive than the LoD values from the DOPC sensor even though they are aligned with the LoD values (Fig. 4 and **Table S1**). The reason for this is that the electrode-supported DOPC monolayer is a very simple platform which records direct interactions of a compound with the single component DOPC layer. On the other hand the *in-vitro* cell-line is a living composite system which has an inherent self-repair mechanism and the assay records breakdown of the cell membrane leading to permeability increase. In addition, other cell membrane constituents aid in maintaining membrane structure and function as the lipid component skeleton itself begins to fail. When the repair mechanism and the other membrane components are overloaded, the cell membrane structure

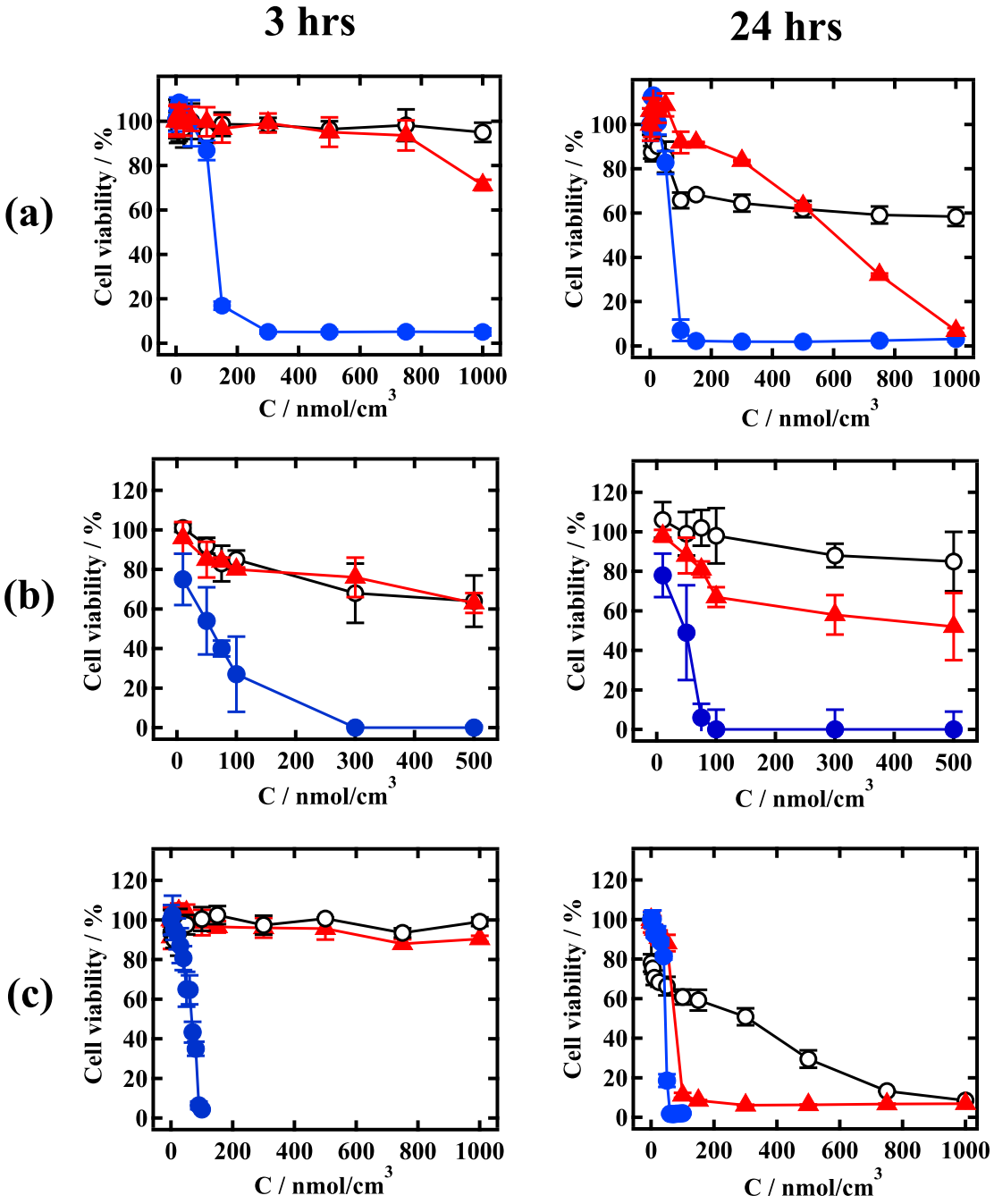

Fig. 3. Dose-response curves of cell viability of, (a) HEK293, (b) Caco-2 TC7, and (c) THP1 cell cultures after exposing to CPZ (blue circles), MMS (red triangles) and COL (unfilled black circles) for 3, 4.5 and 24 hrs as indicated on figure. Data from n = 3 assays are shown as mean ± SD except when error bars are within symbol size. All cell viability results normalised to 100 % at zero toxicant concentration.

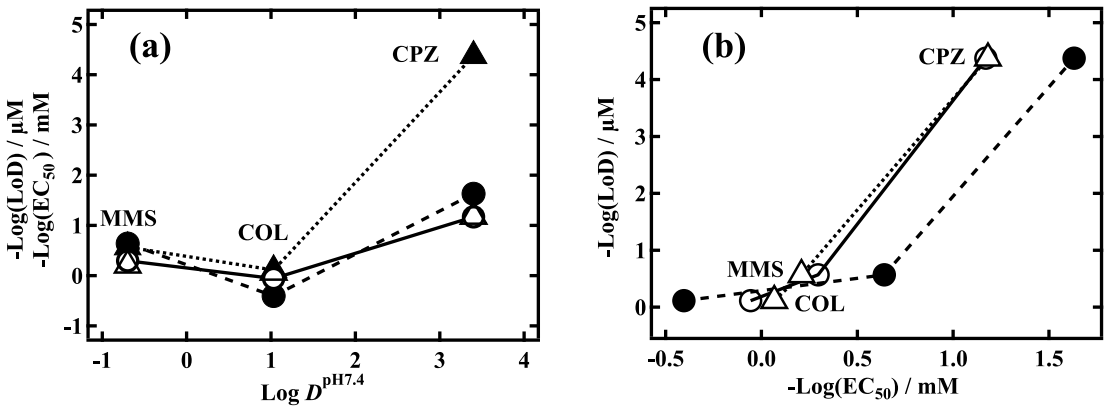

Fig. 4. (a) −Log (LoD)/µM (filled triangle) and –Log (EC_{50})/mM), versus the Log $D^{pH7.4}$ and, (b) −Log (LoD)/µM versus –Log (EC_{50}) / mM from monolayer sensor and cell cultures: HEK293 cells: unfilled triangle, THP1 cells: filled circle, TH1 cells: unfilled circle respectively exposed for 24 hrs to CPZ, MMS and COL as indicated. Data from n = 3 assays are shown as mean ± SD except when error bars are within symbol size.

itself breaks down.

The objective of the analysis in Fig. 4a and indeed in Fig. 5b was to see whether there was any relationship between the membrane activity and acute and non-acute toxicity respectively of the compounds and their lipophilicity as given by log $D^{pH7.4}$. A linear correlation between these two descriptors is often used as an indicator of the biological activity of a drug and/or toxicant. The CPZ toxicity indeed relates to its relatively high log $D^{pH7.4}$ or lipophilicity and correlates with its ability to modify the DOPC layer. Since the action of CPZ on a DOPC layer indicates a positive biomembrane activity of the compound, the molecular initiating event (MIE) of CPZ to the cell lines can be traced to its biomembrane interaction. For the other two compounds, the –log LoD values (and the –log EC_{50} values) are not correlated with the log $D^{pH7.4}$ values which shows that out of the two compounds, the interaction of MMS with the membrane sensor element is facilitated by more factors than lipophilicity alone. MMS is a well-known alkylating agent attacking the phosphate-diester bond in DNA. Previous studies [36] have also suggested that the primary target of MMS is the cell membrane. It is

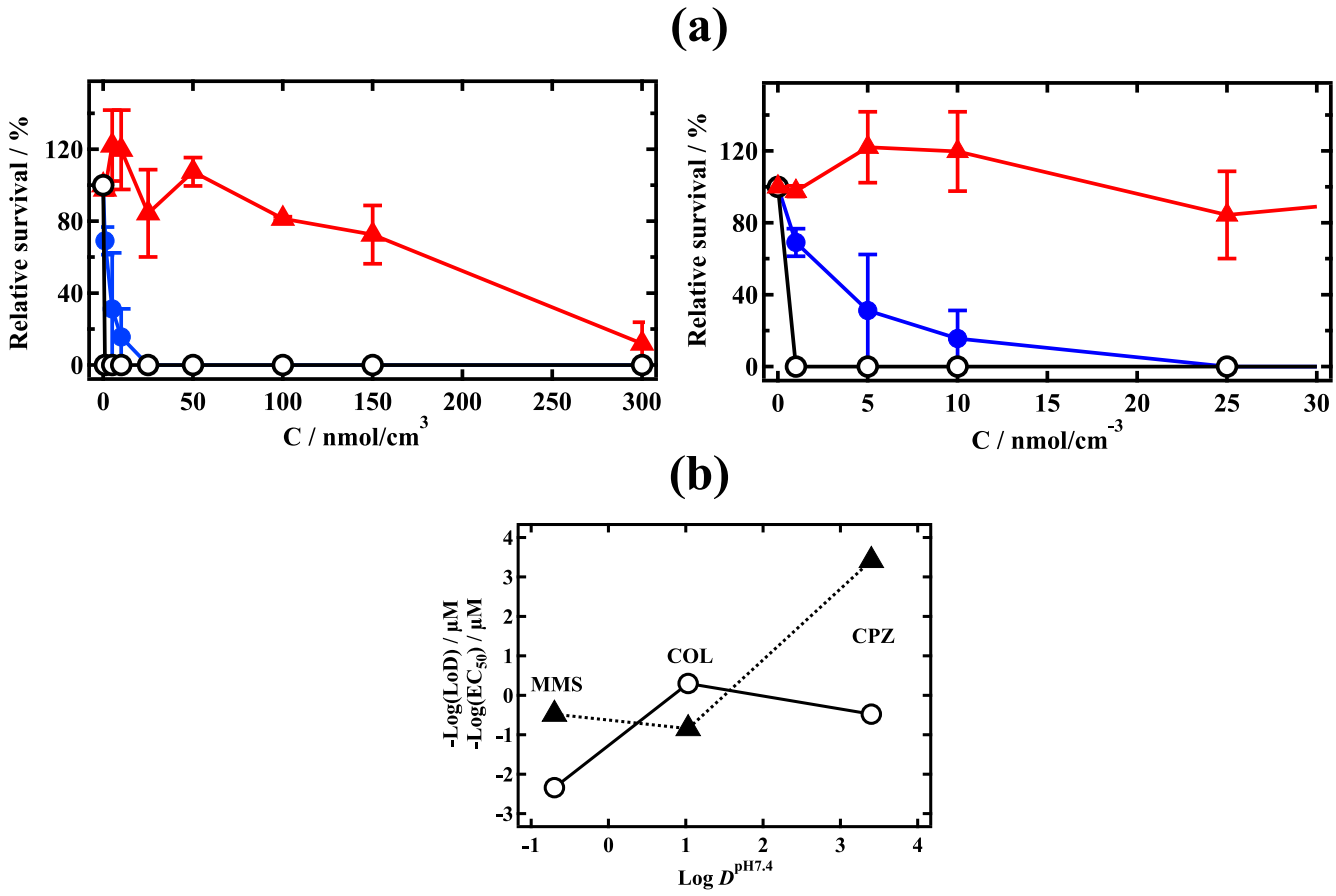

Fig. 5. (a) Cell viability measured by CFE in human lung epithelial cells (A549) after exposure to CPZ (blue filled circles), MMS (red triangles) and COL (black open circles) for 10–12 days versus toxicant concentration, (b) −Log (LoD/µM) measured by DOPC monolayer sensor (filled triangle) and –Log (EC_{50}/µM) (open circle) measured by CFE of human lung epithelial cells (A549) after 10–12 days exposure to MMS, COL and CPZ as indicated on figure versus Log $D^{pH7.4}$. CFE data are presented as mean of two independent experiments with six exposed wells per concentration per experiment.

hypothesised that the delayed effect of MMS is connected with its alkylation of cell line DNA and later induction of cell death. Some interaction with the phospholipid component of the cell membranes may also be possible given the observed interaction of MMS with the DOPC layer. Clearly, attack by MMS on the phosphate-carbon bond in DOPC could instigate this although this reaction has not been shown previously. An interesting additional feature of these results is that the plots and ranking of -Log LoD and – Log EC_{50} versus Log $D^{pH7.4}$ are aligned which can be seen in Fig. 4b.

3.4. Colony forming efficiency in in vitro lung model after exposure to CPZ, MMS and COL

The effect of the three compounds on the colony forming efficiency (CFE) of A549 cell lines is displayed in Fig. 5**a** and **b**. It is observed that the response to COL is effective at the lowest compound concentration within the 10–12-day time scale, whereas that of MMS is significantly less. The response to CPZ falls somewhere in-between. This toxicity ranking can only be understood within the terms of reference of the assay itself. CFE efficiency is a metric of the proliferation potential of cell lines. In this aspect, it differs from the acute viability measurement of cell lines. Accordingly, a toxicant can have an immediate effect on the cell viability *in vitro* through a disruption of their outer membrane for example but the same toxicant will still allow a certain number of cells to divide. Thus, examination of cytotoxicity by AlamarBlue™ (Fig. 3) shows that 2 nmol/cm^3 CPZ kills about 20 % of the cells but allows 80 % to continue dividing. In this way, the CFE assay predominantly measures the cell proliferation or dividing potential of the cells. As a result, the pronounced response of the CFE assay to COL is a reflection of the known action of COL on the mitotic division of cells. The response to CPZ is a consequence of the acute effect of CPZ on the viability of the cells. The weak response to MMS is surprising. Its effect on the viability of the cell lines is delayed to 24 hrs as shown in Fig. 3. However, this delay allows further cells to divide during this time. In fact, it is the delayed influence on the viability of the cells, which allows the cells to continue proliferating at the lower concentrations of MMS.

For the CFE systems, EC_{50} values were calculated from the dose–response curves (Fig. 5**a)** and displayed as plots of –Log (EC_{50}) versus Log $D^{pH7.4}$ (Fig. 5**b**). In contrast to the acute cell viability studies, there is no alignment between the LoD and the EC_{50} for the three compounds since COL shows the maximum activity on cell division over 12–14 days whereas CPZ has the acute maximum activity on the phospholipid layer. In addition, there is no relation between the lipophilicity of the compounds and their effect on cell viability over 12–14 days since lipophilicity is not a critical factor in the interaction of COL on the spindle formation during cell division.

3.5. Genotoxicity screening of CPZ, MMS and COL in human in vitro models

Representative results of the comet assay with two cell lines (THP1 and HEK293) exposed to the test compounds CPZ, MMS or COL for 3 hrs and 24 hrs are displayed in Figs. 6 **and S2**. As expected, the MMS induced DNA strand breakage occurs in a concentration dependent manner. Fig. 6 shows a higher level of DNA breaks after 3 h exposure to MMS compared to 24 h exposure. As MMS reacts by donating methyl

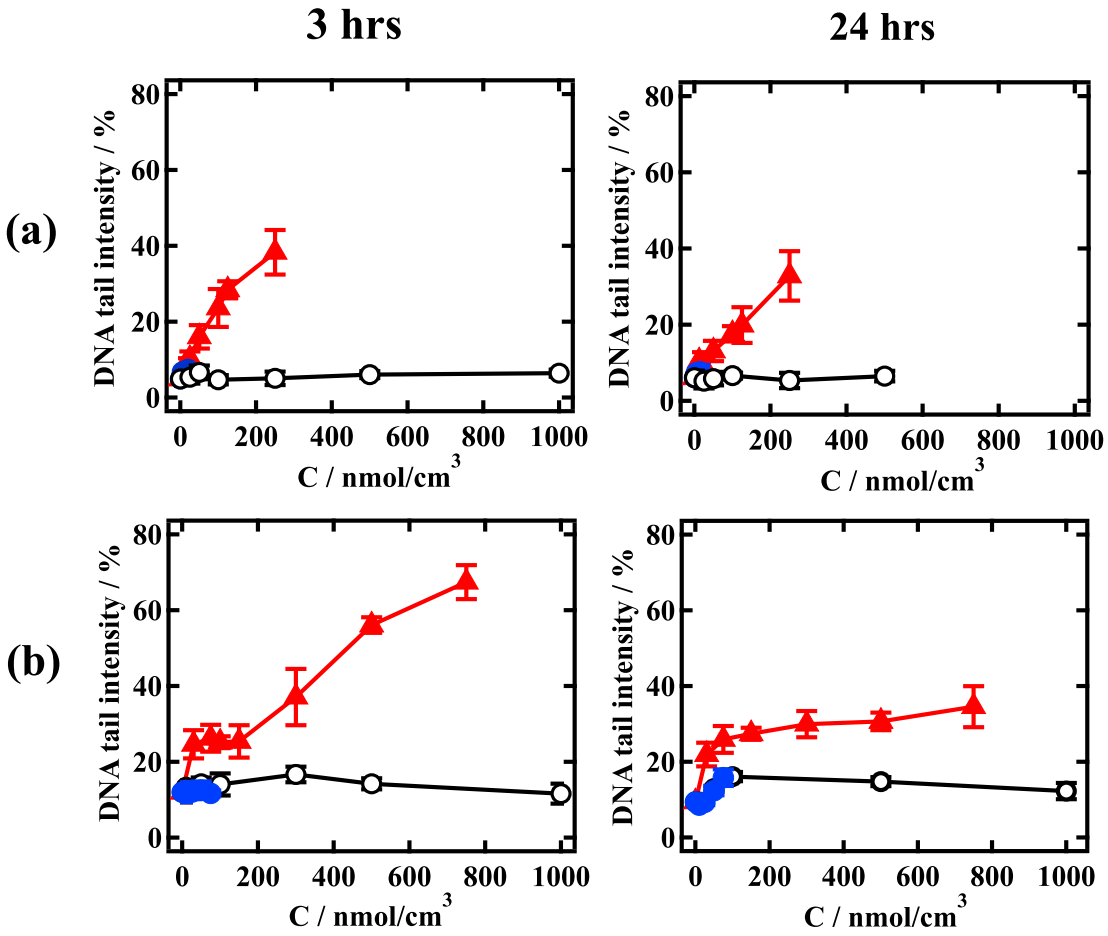

Fig. 6. DNA strand breaks measured as DNA tail intensity by the comet assay after exposure of the following human cell lines (a) THP1 cells and (b) HEK293 cells after 3 hrs and 24 hrs exposure as indicated on diagram to CPZ (blue circles), MMS (red triangles) and COL(unfilled black circles). Data from n = 3 assays are shown as mean ± SD except when error bars are within symbol size.

groups, the more it reacts, the less effective it becomes as an alkylating agent which leads to a small decrease in its concentration. Since DNA repair is occurring throughout the incubation, it is not surprising that the level of DNA damage detected is less after 24 h exposure. No significant DNA damage was detected after exposure to COL. After exposure to CPZ, no DNA damage was detected either, due to a different mechanism leading to cell toxicity before a DNA base lesion could be introduced. It was not possible to observe the response of the DNA to higher concentrations of CPZ since the cell lines had no viability to these levels of compound. Interestingly, the full response to MMS only occurs after 3 hrs, which contrasts with the cell viability response to MMS, which took 24 hrs to progress. This indicates that as assumed earlier the effect of MMS on cell viability is a later consequence of DNA damage as well as due to other possible effects.

4. Conclusions

The validation of a novel Hg-supported DOPC membrane platform for cell-free, toxicity screening of chemicals was carried out by comparing screening results to routine *in vitro* toxicity testing systems.

Results showed:-

1. The membrane sensor response recorded a sensitivity to CPZ which is 6.4×10^3 orders of magnitude greater than MMS, whereas for the cell cultures the same sensitivity was one order of magnitude greater. However, the ranking of the magnitude of membrane sensor response to the toxicants was the same as that of the cell culture viability response and was CPZ > MMS > COL. The membrane sensor element gave a rapid response within 10 min, whereas induction of cell death required up to 24 hrs to give the same rank order.
2. Using CFE as an endpoint showed a toxicity rank order of COL > CPZ > MMS. In this latter case, the end-point is related to the effect of COL on mitotic cell division, which affects cell division over 10–12 days. The Comet Assay showed out of the three toxicants only MMS significantly damages the DNA of A549, HepG2, TH1 and HEK293 cells, which is commensurate with its methylating properties.
3. The similarity between the toxicant's activity ranked acute by cell viability to the electrochemical membrane sensor element's damage indicates that non-specific biomembrane damage inflicted by the toxicant accounts for the activity of the toxicants towards the acute viability of the *in vitro* models.
4. The study showed that the membrane sensor platform is a valid device for rapid *online* cell-free screening of chemicals for acute cytotoxicity where biomembrane damage is the MIE. In addition the phospholipid bilayer skeleton is critical to the structure and functioning of the very much more complex biomembrane Modification and damage to this structure by a toxicant indicates that the same toxicant will undermine the function of a cell outer membrane.

CRediT authorship contribution statement

Yvonne Kohl: Conceptualization, Funding acquisition, Visualization. **Nicola William:** Investigation, Methodology, Visualization. **Elisabeth Elje:** Investigation, Methodology. **Nadine Backes:** Investigation, Methodology. **Mario Rothbauer:** Investigation, Methodology. **Annamaria Srancikova:** Methodology. **Elise Rundén-Pran:** Methodology. **Naouale El Yamani:** Methodology. **Rafi Korenstein:** Funding acquisition. **Lea Madi:** Investigation, Methodology. **Alexander Barbul:** Methodology. **Katarina Kozics:** Investigation, Methodology. **Monika Sramkova:** Investigation, Methodology. **Karen Steenson:** . **Alena Gabelova:** Funding acquisition. **Peter Ertl:** Funding acquisition. **Maria Dusinska:** Funding acquisition. **Andrew Nelson:** Conceptualization, Funding acquisition, Visualization.

Declaration of Competing Interest

The authors declare that they have no known competing financial interests or personal relationships that could have appeared to influence the work reported in this paper.

Data availability

Data will be made available on request.

Acknowledgements

The authors thank Iren E. Sturtzel (NILU) for technical assistance.

This work was supported by the European Commission under the Horizon2020 programmes [grant number 685817 (HISENTS), grant number 862296 (SABYDOMA), grant number 857381 (VISION), grant number 814425 (RiskGONE), and grant number 814572 (NanoSolveIT)].

Appendix A. Supplementary material

Supplementary data to this article can be found online at https://doi.org/10.1016/j.bioelechem.2023.108467.

References

[1] National Research Council, Toxicity testing in the 21st century: A vision and a strategy, The National Academies Press, Washington, DC, 2007 doi:10.17226/11970.
[2] K.U. Goss, K. Bittermann, L. Henneberger, L. Linden, Equilibrium biopartitioning of organic anions – A case study for humans and fish, Chemosphere 199 (2018) 174–181, https://doi.org/10.1016/J.CHEMOSPHERE.2018.02.026.
[3] S. Fujisawa, T. Atsumi, Y. Kadoma, Cytotoxicity of methyl methacrylate (MMA) and related compounds and their interaction with dipalmitoylphosphatidylcholine (DPPC) liposomes as a model for biomembranes, Oral Dis. 6 (2000) 215–221, https://doi.org/10.1111/j.1601-0825.2000.tb00116.x.
[4] B.I. Escher, R.P. Schwarzenbach, Partitioning of substituted phenols in liposome−water, biomembrane−water, and octanol−water systems, Environ. Sci. Technol. 30 (1995) 260–270, https://doi.org/10.1021/ES9503084.
[5] E.U. Ramos, W.H.J. Vaes, H.J.M. Verhaar, J.L.M. Hermens, Quantitative structure−activity relationships for the aquatic toxicity of polar and nonpolar narcotic pollutants, J. Chem. Inf. Comput. Sci. 38 (1998) 845–852, https://doi.org/10.1021/CI980027Q.
[6] A.D. Gunatilleka, C.F. Poole, Models for estimating the non-specific toxicity of organic compounds in short-term bioassays, Analyst 125 (2000) 127–132. www.rsc.org/suppdata/an/a9/a907235g.
[7] H. Glatt, I. Gemperlein, F. Setiabudi, K.L. Platt, F. Oesch, Expression of xenobiotic-metabolizing enzymes in propagatable cell cultures and induction of micronuclei by 13 compounds, Mutagenesis 5 (1990) 241–250. https://academic.oup.com/mutage/article/5/3/241/1179092.
[8] M. Hervé, J.C. Debouzy, E. Borowski, B. Cybulska, C.M. Gary-Bobo, The role of the carboxyl and amino groups of polyene macrolides in their interactions with sterols and their selective toxicity. A 31P-NMR study, accessed January 21, 2022, Biochim. Biophys. Acta - Biomembr. 980 (1989) 261–272, https://www.academia.edu/32989414/The_role_of_the_carboxyl_and_amino_groups_of_polyene_macrolides_in_their_interactions_with_sterols_and_their_selective_toxicity_A_31P_NMR_study.
[9] A. Dahlin, M. Zäch, T. Rindzevicius, M. Käll, D.S. Sutherland, F. Höök, Localized surface plasmon resonance sensing of lipid-membrane-mediated biorecognition events, J. Am. Chem. Soc. 127 (2005) 5043–5048, https://doi.org/10.1021/JA043672O.
[10] N. Gal, D. Malferarri, S. Kolusheva, P. Galletti, E. Tagliavini, R. Jelinek, Membrane interactions of ionic liquids: Possible determinants for biological activity and toxicity, Biochim. Biophys. Acta - Biomembr. 2012 (1818) 2967–2974, https://doi.org/10.1016/J.BBAMEM.2012.07.025.
[11] M.N. Jones, Surfactant interactions with biomembranes and proteins, Chem. Soc. Rev. 21 (1992) 127–136, https://doi.org/10.1039/CS9922100127.
[12] T.W. Sirk, E.F. Brown, M. Friedman, A.K. Sum, Molecular binding of catechins to biomembranes: relationship to biological activity, J. Agric. Food Chem. 57 (2009) 6720–6728, https://doi.org/10.1021/JF900951W/SUPPL_FILE/JF900951W_SI_001.PDF.
[13] C. Pidgeon, S. Ong, H. Liu, X. Qiu, M. Pidgeon, A.H. Dantzig, J. Munroe, W. J. Homback, J.S. Kasher, L. Glunz, T. Szczerba, IAM chromatography: an in vitro screen for predicting drug membrane permeability, J. Med. Chem. 38 (1995) 590–594, https://doi.org/10.1021/JM00004A004.
[14] A. Taillardat-Bertschinger, C.A.M. Martinet, P.-A. Carrupt, M. Reist, G. Caron, R. Fruttero, B. Testa, Molecular factors influencing retention on immobilized artifical membranes (IAM) compared to partitioning in liposomes and n-octanol, Pharm Res. 19 (2002) 729–737.

[15] A. Nelson, Electrochemistry of mercury supported phospholipid monolayers and bilayers, Curr. Opin. Colloid Interface Sci. 15 (2010) 455–466, https://doi.org/10.1016/J.COCIS.2010.07.004.
[16] A. Nelson, N. Auffret, Phospholipid monolayers of di-oleoyl lecithin (di-O-PC) at the mercury/water interface: Effects on faradaic reactions, J. Electroanal. Chem. Interfacial Electrochem. 248 (1988) 167–180, https://doi.org/10.1016/0022-0728(88)85159-3.
[17] A. Nelson, A. Benton, Phospholipid monolayers at the mercury / water interface, J. Electroanal. Chem. Interfacial Electrochem. 202 (1986) 253–270, https://doi.org/10.1016/0022-0728(86)90123-3.
[18] D. Bizzotto, A. Nelson, Continuing electrochemical studies of phospholipid monolayers of dioleoyl phosphatidylcholine at the mercury−electrolyte interface, Langmuir. 14 (1998) 6269–6273, https://doi.org/10.1021/LA980314O.
[19] Z. Coldrick, A. Penezic, P. Penezic, B. Gašparovic, G. Gašparovic, P. Steenson, J. Merrifield, A. Nelson, High throughput systems for screening biomembrane interactions on fabricated mercury film electrodes, J. Appl. Electrochem. 41 (2011) 939–949, https://doi.org/10.1007/s10800-011-0319-7.
[20] Z. Coldrick, P. Steenson, P. Millner, M. Davies, A. Nelson, Phospholipid monolayer coated microfabricated electrodes to model the interaction of molecules with biomembranes, Electrochim. Acta. 54 (2009) 4954–4962, https://doi.org/10.1016/J.ELECTACTA.2009.02.095.
[21] S. Mohamadi, D.J. Tate, A. Vakurov, A. Nelson, Electrochemical screening of biomembrane-active compounds in water, Anal. Chim. Acta. 813 (2014) 83–89, https://doi.org/10.1016/J.ACA.2014.01.009.
[22] A. Vakurov, R. Brydson, A. Nelson, Electrochemical modeling of the silica nanoparticle-biomembrane interaction, Langmuir. 28 (2012) 1246–1255, https://doi.org/10.1021/LA203568N.
[23] N. Ormategui, S. Zhang, I. Loinaz, R. Brydson, A. Nelson, A. Vakurov, Interaction of poly(N-isopropylacrylamide) (pNIPAM) based nanoparticles and their linear polymer precursor with phospholipid membrane models, Bioelectrochemistry 87 (2012) 211–219, https://doi.org/10.1016/J.BIOELECHEM.2011.12.006.
[24] N. William, A. Nelson, S. Gutsell, G. Hodges, J. Rabone, A. Teixeira, Hg-supported phospholipid monolayer as rapid screening device for low molecular weight narcotic compounds in water, Anal. Chim. Acta. 1069 (2019) 98–107, https://doi.org/10.1016/J.ACA.2019.04.019.
[25] A. Nelson, N. Auffret, J. Borlakoglu, Interaction of hydrophobic organic compounds with mercury adsorbed dioleoylphosphatidylcholine monolayers, Biochim. Biophys. Acta - Biomembr. 1021 (1990) 205–216, https://doi.org/10.1016/0005-2736(90)90035-M.
[26] S. De Haan, X. Liu, chlorpromazine dose for people with schizophrenia, Schizophrenia Bull. 35 (2009) 491–492, https://doi.org/10.1093/schbul/sbp014.
[27] M. Kalkanidis, N. Klonis, L. Tilley, L.W. Deady, Novel phenothiazine antimalarials: synthesis, antimalarial activity, and inhibition of the formation of β-haematin, Biochem. Pharmacol. 63 (2002) 833–842, https://doi.org/10.1016/S0006-2952(01)00840-1.
[28] S. Mishra, A.K. Mishra, Effects of chlorpromazine drug on DPPC lipid: Density functional theory study, Int. J. Environ. Anal. Chem. 101 (2019) 1773–1784, https://doi.org/10.1080/03067319.2019.1686497.
[29] T. Ogiso, M. Iwaki, K. Mori, Fluidity of human erythrocyte membrane and effect of chlorpromazine on fluidity and phase separation of membrane, Biochim. Biophys. Acta - Biomembr. 649 (1981) 325–335, https://doi.org/10.1016/0005-2736(81)90422-3.
[30] G.J. Smith, J.W. Grisham, Cytotoxicity of monofunctional alkylating agents methyl methanesulfonate and methyl-N′-nitro-N-nitrosoguanidine have different mechanisms of toxicity for 10T12 cells, Mutat. Res. Mol. Mech. Mutagen. 111 (1983) 405–417, https://doi.org/10.1016/0027-5107(83)90036-2.
[31] M.H.L. Green, A.S.C. Medcalf, C.F. Arlett, S.A. Harcourt, A.R. Lehmann, DNA strand breakage caused by dichlorvos, methyl methanesulphonate and iodoacetamide in Escherichia coli and cultured chinese hamster cells, Mutat. Res. Mol. Mech. Mutagen. 24 (1974) 365–378, https://doi.org/10.1016/0027-5107(74)90181-X.
[32] R. Anindya, Single-stranded DNA damage: Protecting the single-stranded DNA from chemical attack, DNA Repair (Amst). 87 (2020), 102804, https://doi.org/10.1016/J.DNAREP.2020.102804.
[33] F. Calléja, J.G. Jansen, H. Vrieling, F. Laval, A.A. Van Zeeland, Modulation of the toxic and mutagenic effects induced by methyl methanesulfonate in Chinese hamster ovary cells by overexpression of the rat N-alkylpurine-DNA glycosylase, Mutat. Res. Mol. Mech. Mutagen. 425 (1999) 185–194, https://doi.org/10.1016/S0027-5107(99)00034-2.
[34] G.A. Sega, K.W. Wolfe, J. Owens, A comparison of the molecular action of an SN1-Type methylating agent, methyl nitrosourea and an SN2-Type Methylating agent, Methyl Methanesulfonate, in the germ cells of male mice, Chem. Biol. Interact. 33 (1981) 253–269.
[35] Y. Jiang, S. Shan, L. Chi, G. Zhang, X. Gao, H. Li, X. Zhu, J. Yang, Methyl methanesulfonate induces necroptosis in human lung adenoma A549 cells through the PIG-3-reactive oxygen species pathway, Tumor Biol. 37 (2016) 3785–3795, https://doi.org/10.1007/s13277-015-3531-y.
[36] S. Ovejero, C. Soulet, M. Moriel-Carretero, B. Gauthier, D.H. Roukos, A. Fusco, Molecular sciences the alkylating agent methyl methanesulfonate triggers lipid alterations at the inner nuclear membrane that are independent from its DNA-damaging ability, Int. J. Mol. Sci. 22 (2021) 7461, https://doi.org/10.3390/ijms22147461.
[37] M.L. Brown, J.M. Rieger, T.L. Macdonald, Comparative molecular field analysis of colchicine inhibition and tubulin polymerization for combretastatins binding to the colchicine binding site on β-tubulin, Bioorg. Med. Chem. 8 (2000) 1433–1441, https://doi.org/10.1016/S0968-0896(00)00068-7.
[38] B. Bhattacharyya, D. Panda, S. Gupta, M. Banerjee, Anti-mitotic activity of colchicine and the structural basis for its interaction with tubulin, Med Res Rev. 28 (2007) 155–183, https://doi.org/10.1002/med.20097.
[39] D.A. Skoufias, L. Wilson, Mechanism of inhibition of microtubule polymerization by colchicine: inhibitory potencies of unliganded colchicine and tubulin-colchicine complexes, Biochemistry 31 (1992) 738–746, https://doi.org/10.1021/BI00118A015.
[40] C.A. Iacobuzio-Donahue, E.L. Lee, S.C. Abraham, J.H. Yardley, T.T. Wu, Colchicine toxicity: distinct morphologic findings in gastrointestinal biopsies, Am. J. Surg. Pathol. 25 (2001) 1067–1073, https://doi.org/10.1097/00000478-200108000-00012.
[41] Y.Y. Leung, L.L. Yao Hui, V.B. Kraus, Colchicine—Update on mechanisms of action and therapeutic uses, Semin. Arthritis Rheum. 45 (2015) 341–350, https://doi.org/10.1016/J.SEMARTHRIT.2015.06.013.
[42] J. Owen, M. Kuznecovs, R. Bhamji, N. William, N. Domenech-Garcia, M. Hesler, T. Knoll, Y. Kohl, A. Nelson, N. Kapur, High-throughput electrochemical sensing platform for screening nanomaterial-biomembrane interactions, Cite as Rev. Sci. Instrum. 91 (2020) 25002, https://doi.org/10.1063/1.5131562.
[43] Z. Coldrick, A. Penezić, B. Gašparović, P. Steenson, J. Merrifield, A. Nelson, High throughput systems for screening biomembrane interactions on fabricated mercury film electrodes, J. Appl. Electrochem. 41 (2011) 939–949, https://doi.org/10.1007/s10800-011-0319-7.
[44] E. Elje, M. Hesler, E. Rundén-Pran, P. Mann, E. Mariussen, S. Wagner, M. Dusinska, Y. Kohl, The comet assay applied to HepG2 liver spheroids, Mutat. Res. - Genet. Toxicol. Environ. Mutagen. 845 (2019), 403033, https://doi.org/10.1016/j.mrgentox.2019.03.006.
[45] A. Nelson, F.A.M. Leermakers, Substrate-induced structural changes in electrode-adsorbed lipid layers. Experimental evidence from the behaviour of phospholipid layers on the mercury-water interface, J. Electroanal. Chem. 278 (1990) 73–83, https://doi.org/10.1016/0022-0728(90)85124-N.
[46] A.V. Brukhno, A. Akinshina, Z. Coldrick, A. Nelson, S. Auer, Phase phenomena in supported lipid films under varying electric potential, Soft Matter 7 (2011) 1006–1017, https://doi.org/10.1039/c0sm00724b.
[47] A. Vakurov, M. Galluzzi, A. Podestà, N. Gamper, A.L. Nelson, S.D.A. Connell, Direct characterization of fluid lipid assemblies on mercury in electric fields, ACS Nano. 8 (2014) 3242–3250, https://doi.org/10.1021/NN4037267.
[48] A. Rashid, A. Vakurov, A. Nelson, Role of electrolyte in the occurrence of the voltage induced phase transitions in a dioleoyl phosphatidylcholine monolayer on Hg, Electrochim. Acta. 155 (2015) 458–465, https://doi.org/10.1016/J.ELECTACTA.2014.12.077.
[49] L. Becucci, S. Martinuzzi, E. Monetti, R. Mercatelli, F. Quercioli, D. Battistel, R. Guidelli, Electrochemical impedance spectroscopy and fluorescence lifetime imaging of lipid mixtures self-assembled on mercury, Soft Matter. 6 (2010) 2733–2741, https://doi.org/10.1039/b923895f.
[50] L. Becucci, R. Guidelli, F. Polo, F. Maran, Interaction of mixed-ligand monolayer-protected Au144 clusters with biomimetic membranes as a function of the transmembrane potential, Langmuir. 30 (2014) 8141–8151, https://doi.org/10.1021/LA500909J/SUPPL_FILE/LA500909J_SI_001.PDF.
[51] X. Wang, S. Ma, Y. Su, Y. Zhang, H. Bi, L. Zhang, X. Han, High impedance droplet-solid interface lipid bilayer membranes, Anal. Chem. 87 (2015) 2094–2099, https://doi.org/10.1021/AC502953V.
[52] Y. Kohl, G.J. Oostingh, A. Sossalla, A. Duschl, H. Von Briesen, H. Thielecke, Biocompatible micro-sized cell culture chamber for the detection of nanoparticle-induced IL8 promoter activity on a small cell population, Nanosc. Res. Lett. 6 (2011) 505, https://doi.org/10.1186/1556-276X-6-505.
[53] M. Rothbauer, C. Eilenberger, S. Spitz, B. Bachmann, J. Pajenda, A. Schwaighofer, G. Höll, P.S. Helmke, Y. Kohl, B. Lendl, P. Ertl, FTIR spectroscopy as a novel analytical approach for investigation of glucose transport and glucose transport inhibition studies in transwell in vitro barrier models, Spectrochim. Acta - Part A Mol. Biomol. Spectrosc. 237 (2020), 118388, https://doi.org/10.1016/j.saa.2020.118388.
[54] L. Horev-Azaria, G. Baldi, D. Beno, D. Bonacchi, U. Golla-Schindler, J. C. Kirkpatrick, S. Kolle, R. Landsiedel, O. Maimon, P.N. Marche, J. Ponti, R. Romano, F. Rossi, D. Sommer, C. Uboldi, R.E. Unger, C. Villiers, R. Korenstein, Predictive Toxicology of cobalt ferrite nanoparticles: Comparative in-vitro study of different cellular models using methods of knowledge discovery from data, Part. Fibre Toxicol. 10 (2013) 1–17, https://doi.org/10.1186/1743-8977-10-32.
[55] M. Sramkova, K. Kozics, V. Masanova, I. Uhnakova, F. Razga, V. Nemethova, P. Mazancova, L. Kapka-Skrzypczak, M. Kruszewski, M. Novotova, V.F. Puntes, A. Gabelova, Kidney nanotoxicity studied in human renal proximal tubule epithelial cell line TH1, Mutat. Res. Toxicol. Environ. Mutagen. 845 (2019), 403017, https://doi.org/10.1016/J.MRGENTOX.2019.01.012.
[56] J. O'brien, I. Wilson, T. Orton, F.Ë. Ois Pognan, Investigation of the Alamar Blue (resazurin) fluorescent dye for the assessment of mammalian cell cytotoxicity, Eur. J. Biochem. 267 (2000) 5421–5426, https://doi.org/10.1046/j.1432-1327.2000.01606.x.
[57] M. Boncler, M. Rózalski, U. Krajewska, A. Podswdek, C. Watala, Comparison of PrestoBlue and MTT assays of cellular viability in the assessment of anti-proliferative effects of plant extracts on human endothelial cells, J. Pharmacol. Toxicol. Methods. 69 (2014) 9–16, https://doi.org/10.1016/J.VASCN.2013.09.003.
[58] J. Ponti, R. Colognato, H. Rauscher, S. Gioria, F. Broggi, F. Franchini, C. Pascual, G. Giudetti, F. Rossi, Colony forming efficiency and microscopy analysis of multi-wall carbon nanotubes cell interaction, Toxicol. Lett. 197 (2010) 29–37, https://doi.org/10.1016/J.TOXLET.2010.04.018.

[59] N. El Yamani, A. Collins, E. Rundén-Pran, L.M. Fjellsbø, S. Shaposhnikov, S. Zienolddiny, M. Dusinska, In vitro genotoxicity testing of four reference metal nanomaterials, titanium dioxide, zinc oxide, cerium oxide and silver: towards reliable hazard assessment, Mutagenesis 32 (2017) 117–126, https://doi.org/10.1093/mutage/gew060.

[60] P. Møller, A. Azqueta, E. Boutet-Robinet, G. Koppen, S. Bonassi, M. Milić, G. Gajski, S. Costa, J.P. Teixeira, C. Costa Pereira, M. Dusinska, R. Godschalk, G. Brunborg, K. B. Gutzkow, L. Giovannelli, M.S. Cooke, E. Richling, B. Laffon, V. Valdiglesias, N. Basaran, C. Del Bo', B. Zegura, M. Novak, H. Stopper, P. Vodicka, S. Vodenkova, V.M. de Andrade, M. Sramkova, A. Gabelova, A. Collins, S.A.S. Langie, Minimum information for reporting on the comet assay (MIRCA): recommendations for describing comet assay procedures and results, Nat. Protoc. 15 (2020) 3817–3826, https://doi.org/10.1038/s41596-020-0398-1.

[61] M. Dusinska, J. Tulinska, N. El Yamani, M. Kuricova, A. Liskova, E. Rollerova, E. Rundén-Pran, B. Smolkova, Immunotoxicity, genotoxicity and epigenetic toxicity of nanomaterials: New strategies for toxicity testing? Food Chem. Toxicol. 109 (2017) 797–811, https://doi.org/10.1016/j.fct.2017.08.030.

[62] L. Bálintová, M. Matúšková, A. Gábelová, The evaluation of the efficacy and potential genotoxic hazard of combined SAHA and 5-FU treatment in the chemoresistant colorectal cancer cell lines, Mutat. Res. Toxicol. Environ. Mutagen. 874–875 (2022), 503445, https://doi.org/10.1016/J.MRGENTOX.2022.503445.

[63] N. El Yamani, E. Rundén-Pran, A.R. Collins, E.M. Longhin, E. Elje, P. Hoet, I. Vinković Vrček, S.H. Doak, V. Fessard, M. Dusinska, The miniaturized enzyme-modified comet assay for genotoxicity testing of nanomaterials, Front. Toxicol. 4 (2022) 1–14, https://doi.org/10.3389/ftox.2022.986318.

[64] A. Azqueta, A.M.S. Abdulwahed, A.L. De Cerain, A. Dahwan, A.K. Pandey, A. Collins, A. Lewies, A. Lewinska, B. Engelward, B. Laffon, B. Zegura, C. Ladeira, C. Costa, Measuring DNA modi fi cations with the comet assay : a compendium of protocols, Nat. Protoc. 18 (2023) 929–989, https://doi.org/10.1038/s41596-022-00754-y.

[65] T.D. Bergazin, N. Tielker, Y. Zhang, J. Mao, M.R. Gunner, K. Francisco, C. Ballatore, S.M. Kast, D.L. Mobley, Evaluation of log P, pK_a, and log *D* predictions from the SAMPL7 blind challenge, J. Comput-Aid. Mol. Des. 35 (2021) 771–802, https://doi.org/10.1007/s10822-021-00397-3.

[66] B. Slater, A. McCormack, A. Avdeef, J.E.A. Comer, PH-Metric log P. 4. Comparison of partition coefficients determined by HPLC and potentiometric methods to literature values, J. Pharm. Sci. 83 (1994) 1280–1283, https://doi.org/10.1002/JPS.2600830918.

[67] W.M. Meylan, P.H. Howard, Atom/fragment contribution method for estimating octanol–water partition coefficients, J. Pharm. Sci. 84 (1995) 83–92, https://doi.org/10.1002/JPS.2600840120.

[68] I.M. Abdulbaqi, Y. Darwis, N.A.K. Khan, R.A. Assi, G.O.K. Loh, A Simple (Hplc–Uv) method for the quantification of colchicine in bulk and ethosomal gel nano-formulation and its validation, Int. J. Pharm. Pharm. Sci. 9 (2017) 72–78, https://doi.org/10.22159/ijpps.2017v9i7.18336.